J. Fluid Mech. (1999), *vol.* 399, *pp.* 335–353. Printed in the United Kingdom

© 1999 Cambridge University Press

The current-modified nonlinear Schrödinger equation

By J. R. STOCKER AND D. H. PEREGRINE†

School of Mathematics, University of Bristol, University Walk, Bristol BS8 1TW, UK

(Received 22 March 1999 and in revised form 2 August 1999)

By comparison with both experimental and numerical data, Dysthe's (1979) $O(\epsilon^4)$ modified nonlinear Schrödinger equation has been shown to model the evolution of a slowly varying wavetrain well (here ϵ is the wave steepness). In this work, we extend the equation to include a prescribed, large-scale, $O(\epsilon^2)$ surface current which varies about a mean value. As an introduction, a heuristic derivation of the $O(\epsilon^3)$ current-modified equation, used by Bakhanov *et al.* (1996), is given, before a more formal approach is used to derive the $O(\epsilon^4)$ equation. Numerical solutions of the new equations are compared in one horizontal dimension with those from a fully nonlinear solver for velocity potential in the specific case of a sinusoidal surface current, such as may be due to an underlying internal wave. The comparisons are encouraging, especially for the $O(\epsilon^4)$ equation.

1. Introduction

The effect of a surface current on propagating surface gravity waves is of interest. One may wish to 'read' the surface pattern (by eye, or using radar) and determine the current strength and direction below. The interaction between water waves and currents has been the subject of two substantial reviews: Peregrine (1976) discusses many topics including a section on both large- and small-scale currents and Jonsson (1990) concentrates more on the effects of currents in ocean and coastal areas.

Here we consider surface waves that are short compared with the length scale of the surface current field. Hence, we are able to assume that the wave properties are generally slowly varying. The typical simple model for such short-wave/high-frequency circumstances is that of 'ray' or 'geometric' theory. Although we discuss such solutions, the main thrust of this paper is to present a better model which allows for steeper waves with the scope for good description of somewhat shorter modulations.

The first set of complete equations to describe short waves propagating over much larger scale non-uniform currents were given by Longuet-Higgins & Stewart (1964). Wave energy is not conserved and the concept of 'radiation stress' was introduced to describe the averaged momentum flux terms which govern the interchange of momentum with the current. In this present work, we assume that the effect of this momentum transfer on the form of the surface current is negligible. Following Whitham's (1965, 1967) development of a method of averaging for nonlinear waves, and the use of an averaged Lagrangian, Bretherton & Garrett (1968) developed the

† Author to whom correspondence should be addressed: e-mail: d.h.peregrine@bris.ac.uk.

concept of wave action. Wave action is conserved for many non-dissipative systems where waves interact with currents.

The motivation for this work was to continue the study of internal waves and currents – see Donato, Peregrine & Stocker (1999, hereafter referred to as DPS) for further discussion. In summary, for a simple but representative initial condition, we made a detailed investigation into the effect of two-dimensional interaction between long internal waves and short surface waves of initially uniform wavenumber. Linear ray theory was used to investigate the effect of differing currents and shorter waves on the time and positioning of the focus of the waves. Also, fully nonlinear solutions have been compared with results from the linear ray theory, and an investigation into time of breaking (an essentially nonlinear phenomena) was made using the fully nonlinear code.

The nonlinear Schrödinger (NLS) equation governs the modulations of weakly nonlinear water waves. The derivation of the NLS equation also includes an assumption that wave properties must be slowly varying; this is similar to ray theory, but corresponds to an improved approximation, as long as the waves do not vary greatly from a fixed mean value of wavenumber and frequency, in contrast to the ray theory, where wavenumber and frequency can vary significantly on the larger scale. The standard NLS equation is valid to $O(\epsilon^3)$, where $\epsilon = ak$, the wave steepness, is taken as a small parameter. More than one method can be used to derive the NLS equation for deep water waves. Yuen & Lake (1982) used an averaged Lagrangian method, Zakharov (1968) used a spectral method and Hasimoto & Ono (1972) and Davey & Stewartson (1974) used a multiple scales method. Dysthe (1979) extends the $O(\epsilon^3)$ equation to the 'modified nonlinear Schrödinger equation' (MNLS), which is valid to $O(\epsilon^4)$ for deep water waves, using a multiple scales approach. This form of the NLS takes account of the small mean flow brought about by the radiation stresses of the modulated wavetrain. The potential due to this induced deep water current is of $O(\epsilon^2)$, and in the present work we force the system with a large-scale, slowly varying velocity potential of $O(\epsilon)$, which gives a current of $O(\epsilon^2)$. Brinch-Nielsen, in her thesis (1985), discusses the Dysthe (1979) paper in detail, considering all Fourier modes and finds one minor discrepancy (aside from typographical errors), as well as consistent forms for the resultant surface elevation in terms of the complex amplitude of the wave potential, B, obtained from the nonlinear Schrödinger equation. This thesis is useful for comparison purposes.

Previous work with this approach to wave–current interactions includes Bakhanov *et al.* (1996) which briefly introduces the $O(\epsilon^3)$ current-modified nonlinear Schrödinger equation in one horizontal dimension (with a sinusoidal current) and gives details of an example in two horizontal dimensions, with a submerged moving point dipole. Bakhanov *et al.* (1997) compared results from the $O(\epsilon^3)$ equation to experiment, with initial findings that are encouraging.

Trulsen & Dysthe (1996) extended the $O(\epsilon^4)$ MNLS equation to apply to waves with a broader bandwidth. Specifically, the standard $O(\epsilon^3)$ and $O(\epsilon^4)$ equations are valid for $|\Delta \boldsymbol{k}|/k = O(\epsilon)$, where $|\Delta \boldsymbol{k}|$ is a modulation wavenumber vector and k is the magnitude of the wavenumber vector $\boldsymbol{k}$. The broader bandwidth equation is valid for $|\Delta \boldsymbol{k}|/k = O(\epsilon^{1/2})$ making it more suitable for application to a realistic three-dimensional ocean wave spectrum. The broader bandwidth terms do not affect the one-dimensional solutions, i.e. the (x, t) equation.

There are a number of numerical methods for solving the NLS equation. Lo & Mei (1985) published a method to solve Dysthe's $O(\epsilon^4)$ equation and compared their results with experiment. Weidman & Herbst (1986) used a split-step method to

solve the $O(\epsilon^3)$ equation, using both a Fourier method (applicable only to periodic problems) and a finite difference method (which can be used for problems set in non-periodic domains). These methods are employed to solve the current-modified NLS equations derived here. It should be noted that Ablowitz & Herbst (1990) warn that non-physical chaotic behaviour may occur when numerical approximations are insufficiently accurate.

The fully nonlinear two-dimensional potential flow problem corresponding to the one-dimensional NLS equations, may be solved numerically using a boundary integral method. The code of Dold & Peregrine (1986) and Dold (1992), which applies this method, has been adapted to include a potential to generate a periodic surface current, as described in DPS, and these results are useful for comparison with numerical solutions of the current-modified nonlinear Schrödinger equation. We present results from these calculations.

In the present paper we take as an example of a surface current that due to an internal wave which may have been caused by tidal flow over the edge of the continental shelf, or else on a smaller scale, by flow in estuarine regions. These internal waves are approximately periodic and therefore generate periodic surface currents, which are sinusoidal if the internal wave is taken to be linear. The surface waves are assumed to be sufficiently short that they are unaffected by any stratification of water density, or vertical variation of current or water depth.

In § 2, a heuristic derivation of the $O(\epsilon^3)$ current-modified NLS equation is presented, following a method discussed by Yuen & Lake (1982). In § 3, a more formal approach is adopted following Dysthe (1979) and Brinch-Nielsen (1985) to derive the $O(\epsilon^4)$ current-modified equation. In § 4 a specific current is considered and the range of validity of the equations discussed. Results showing comparison of surface profiles with fully nonlinear results in one horizontal dimension are given in § 5. A discussion of when the equation is valid is included. Our conclusions are given in § 6. The Appendix gives further details of the derivation of the $O(\epsilon^4)$ current-modified NLS equation.

2. Derivation of the $O(\epsilon^3)$ evolution equation

Consider perturbations from a carrier wave with frequency ω_0 and wavenumber vector $\boldsymbol{k}_0$. We take a slowly varying, periodic current $\boldsymbol{U}(\boldsymbol{x}, t)$ and consider perturbations from a fixed value of the current $\overline{\boldsymbol{U}} = (U_0, V_0)$. The dispersion relation for the carrier wave on the basic current then takes the form

$$\omega_0 = \overline{\boldsymbol{U}} \cdot \boldsymbol{k}_0 \pm \sigma(k_0), \tag{1}$$

where $k_0 = |\boldsymbol{k}_0|$, and $\sigma(k_0)$ is the frequency of the carrier wave relative to a reference frame moving with the water. The positive root in equation (1) is chosen so as to select waves travelling relative to the water in the positive $\boldsymbol{k}_0$ direction at speed $c_0 = +(g/k_0)^{1/2}$. Consider weakly nonlinear perturbations to this wavetrain such that $\epsilon = ak \ll 1$ where a is wave amplitude, $\boldsymbol{k}$ is the wavenumber and $k = |\boldsymbol{k}|$. The frequency, ω and wavenumber are then governed by the relation

$$\omega = \boldsymbol{U} \cdot \boldsymbol{k} + (gk)^{1/2} \left[1 + \tfrac{1}{2}(ak)^2 + O((ak)^4)\right], \tag{2}$$

where Stokes relation for the frequency dispersion has been used (for example see Lamb 1932). The frequency and wavenumber are expanded to first order in terms of ϵ, and the current $\boldsymbol{U}$ is given an $O(\epsilon^2)$ perturbation, described by

$$\omega = \omega_0 + \omega_1, \qquad \boldsymbol{k} = k_0 \boldsymbol{i} + (l, m) \quad \text{and} \quad \boldsymbol{U} = \overline{\boldsymbol{U}} + (U_1(\boldsymbol{x}, t), V_1(\boldsymbol{x}, t)), \tag{3}$$

where ω_1, l and m are $O(\epsilon)$ and U_1, V_1 are $O(\epsilon^2)$. Including terms up to $O(\epsilon^2)$, we obtain

$$\omega_1 - c_{g0}l - U_0 l - V_0 m + \frac{(gk_0)^{1/2}}{k_0^2}\left(\tfrac{1}{8}l^2 - \tfrac{1}{4}m^2\right) - \frac{k_0^2(gk_0)^{1/2}}{2}a^2 - k_0 U_1 = O(\epsilon^3). \quad (4)$$

The group velocity of the carrier wave in the absence of a current is $c_{g0} = \frac{1}{2}(g/k_0)^{1/2}$. Following Yuen & Lake's (1982) method, we make the direct correspondence

$$\omega_1 = \mathrm{i}\frac{\partial}{\partial t}, \qquad -l = \mathrm{i}\frac{\partial}{\partial x} \quad \text{and} \quad -m = \mathrm{i}\frac{\partial}{\partial y} \quad (5)$$

which can be made rigorous for a linear, homogeneous wave system of uniform properties. However, when we are including a non-uniform current, the second and third relationships of (5) are not accurate unless ∇U_1 and ∇V_1 are negligible; the rigorous analysis in the next section shows that this is indeed the case for the expansion in equation (3). The correspondence (5) and equation (4) lead to the operator

$$\mathbf{P} = \mathrm{i}\left[\frac{\partial}{\partial t} + c_{g0}\frac{\partial}{\partial x} + U_0\frac{\partial}{\partial x} + V_0\frac{\partial}{\partial y}\right] - \frac{(gk_0)^{1/2}}{k_0^2}\left[\frac{1}{8}\frac{\partial^2}{\partial x^2} - \frac{1}{4}\frac{\partial^2}{\partial y^2}\right] - \frac{k_0^2(gk_0)^{1/2}}{2}a^2 - k_0 U_1, \quad (6)$$

which can be applied to the complex wave envelope A so that $\mathbf{P}(A) = 0$. In the frame of reference moving with velocity $(c_{g0} + U_0, V_0)$, we have

$$\mathrm{i}A_t - \frac{(gk_0)^{1/2}}{k_0^2}\left[\tfrac{1}{8}A_{XX} - \tfrac{1}{4}A_{YY}\right] - \frac{k_0^2(gk_0)^{1/2}}{2}A|A|^2 - k_0 U_1 A = 0, \quad (7)$$

where $X = x - \{c_{g0} + U_0\}t$, $Y = y - V_0 t$ and the suffix notation for derivatives has been adopted.

It is sensible to make the amplitude, length and time scales dimensionless using the length and time scales respectively of the carrier wave. So, defining $\overline{A} = k_0 A$, $\overline{X} = k_0 X$, $\overline{Y} = k_0 Y$ and $T = (gk_0)^{1/2}t$, equation (7) is replaced by

$$\mathrm{i}\overline{A}_T - \tfrac{1}{8}\overline{A}_{\overline{X}\,\overline{X}} + \tfrac{1}{4}\overline{A}_{\overline{Y}\,\overline{Y}} - \tfrac{1}{2}\overline{A}|\overline{A}|^2 - f(\overline{X}, \overline{Y}, T)\overline{A} = 0 \quad (8)$$

where $f(\overline{X}, \overline{Y}, T)$ is the x-component of the non-dimensional current variation. This reduces equation (8) to a standard form of the NLS when $\boldsymbol{U} \equiv 0$.

As is the case in the absence of a current, we find that for steeper waves, equation (8) does not accurately model the nonlinear interactions; in particular it does not give a good prediction for the speed of wave groups. We therefore extend the equation to a higher order in wave steepness, $\epsilon = ak$, which includes the small mean flow brought about by radiation stresses of the modulated wavetrain, as well as further terms involving the large-scale surface current.

3. Higher-order terms (up to $O(\epsilon^4)$)

In order to model steeper and shorter wave packets, we consider higher-order terms in the expansion, and take a more formal approach to the analysis. Let ϕ be the velocity potential for the flow and ζ the corresponding surface elevation. We basically follow Dysthe (1979) but also take note of the work by Brinch-Nielsen (1985) who studied the Dysthe analysis in detail and found minor discrepancies. Brinch-Nielsen used the Bernoulli equation in place of Dysthe's equation (2.3) and we follow this approach as the analysis is simplified somewhat. Our equations are considered in a

frame of reference moving with velocity $\overline{\boldsymbol{U}}$, which is constant and taken to be $-\boldsymbol{V}$. The governing equations for the flow, in which waves and current are taken to be irrotational so that we can work with a velocity potential, are

$$z \leqslant \zeta, \quad \nabla^2\phi = 0, \tag{9}$$

$$z = \zeta, \quad \left(\frac{\partial}{\partial t} - \boldsymbol{V}\cdot\nabla_h\right)^2 \phi + g\frac{\partial\phi}{\partial z} + \left(\frac{\partial}{\partial t} - \boldsymbol{V}\cdot\nabla_h\right)(\nabla\phi)^2 + \tfrac{1}{2}\nabla\phi\cdot\nabla(\nabla\phi)^2 = 0, \tag{10}$$

$$z = \zeta, \quad \left(\frac{\partial}{\partial t} - \boldsymbol{V}\cdot\nabla_h\right)\phi + g\zeta + \tfrac{1}{2}(\nabla\phi)^2 = 0, \tag{11}$$

$$z \to -\infty, \quad \frac{\partial\phi}{\partial z} = 0, \tag{12}$$

where g is acceleration due to gravity and z is the vertical coordinate measured downwards from the equilibrium position. Equation (9) is Laplace's equation, (10) is a combined form of the Bernoulli and kinematic boundary conditions at the free surface which is convenient to use as it does not involve ζ explicitly, and (11) is the surface pressure condition, using the Bernoulli equation. The expressions in (10) and (11) are expanded as a Taylor series about $z = 0$ in order to give values at $z = \zeta$, using the fact that $\zeta = O(\epsilon)$. As equation (10) is used to derive the governing equation for the complex potential, B, terms up to and including $O(\epsilon^4)$ are included whereas equation (11) is used to obtain an expression for ζ, the surface elevation, so terms up to and including $O(\epsilon^3)$ are kept. In equations (10) and (11), ∇_h represents $(\partial/\partial x, \partial/\partial y)$. Equations (10) and (11) become

$$z = 0, \quad \mathrm{L}\phi + \zeta\mathrm{L}\frac{\partial\phi}{\partial z} + \left(\frac{\partial}{\partial t} - \boldsymbol{V}\cdot\nabla_h\right)(\nabla\phi)^2 + Q_3 + Q_4 = O(\epsilon^5) \tag{13}$$

$$z = 0, \quad \left(\frac{\partial}{\partial t} - \boldsymbol{V}\cdot\nabla_h\right)\phi + g\zeta + \zeta\frac{\partial}{\partial z}\left(\frac{\partial}{\partial t} - \boldsymbol{V}\cdot\nabla_h\right)\phi + \tfrac{1}{2}(\nabla\phi)^2 + R_3 = O(\epsilon^4) \tag{14}$$

where

$$\mathrm{L} = \left(\frac{\partial}{\partial t} - \boldsymbol{V}\cdot\nabla_h\right)^2 + g\frac{\partial}{\partial z},$$

$$Q_3 = \tfrac{1}{2}\zeta^2\mathrm{L}\frac{\partial^2\phi}{\partial z^2} + \tfrac{1}{2}\nabla\phi\cdot\nabla(\nabla\phi)^2 + \zeta\left(\frac{\partial}{\partial t} - \boldsymbol{V}\cdot\nabla_h\right)\frac{\partial}{\partial z}(\nabla\phi)^2,$$

$$R_3 = \tfrac{1}{2}\zeta^2\frac{\partial^2}{\partial z^2}\left(\frac{\partial}{\partial t} - \boldsymbol{V}\cdot\nabla_h\right)\phi + \tfrac{1}{2}\zeta\frac{\partial}{\partial z}(\nabla\phi)^2,$$

and Q_4 is a term of $O(\epsilon^4)$, omitted in Dysthe (1979), which is given explicitly in the Appendix.

Let the velocity potential ϕ and surface elevation ζ be expanded as

$$\phi = \bar{\phi} + \phi_c + \tfrac{1}{2}\left[B\mathrm{e}^{k_0 z}\mathrm{e}^{\mathrm{i}\theta} + B_2\mathrm{e}^{2k_0 z}\mathrm{e}^{2\mathrm{i}\theta} + \text{c.c.}\right] \tag{15}$$

and

$$\zeta = \bar{\zeta} + \zeta_c + \tfrac{1}{2}\left[A\mathrm{e}^{\mathrm{i}\theta} + A_2\mathrm{e}^{2\mathrm{i}\theta} + A_3\mathrm{e}^{3\mathrm{i}\theta} + \text{c.c.}\right], \tag{16}$$

where $\theta = k_0 x - \omega_0 t$ and c.c. denotes complex conjugate, thus making both ϕ and ζ real. Note that we use a form for the complex potential B and amplitude A which is

consistent with the derivation in § 2, and differs from that used in Dysthe (1979) by a factor of two. In the following multiple-scales analysis, B and A are both of order ϵ and differentiation of B and A with respect to x, y, z or t decreases their order of magnitude by one. For example, $\partial A/\partial t$ is $O(\epsilon^2)$ and $\partial^3 B/\partial y^2 \partial x$ is $O(\epsilon^4)$. Factors of ϵ, which indicate the magnitude of terms explicitly, have been omitted in the expansions for brevity, as in Dysthe (1979). The potential $\bar{\phi}$ represents the mean flow brought about by the radiation stress of the wave and ϕ_c gives the surface current; $\bar{\zeta}$ and ζ_c are the corresponding surface elevations. Dysthe, in his analysis, found that $\bar{\phi}$ was of order ϵ^2. We follow his analysis including the potential due to the large-scale current, which we take to be $O(\epsilon)$. As in Brinch-Nielsen, we find B_2 to be $O(\epsilon^4)$, so we use this fact to neglect the intermediate $O(\epsilon^2)$ and $O(\epsilon^3)$ terms to simplify the presentation of the analysis.

The surface current potential satisfies Laplace's equation in the fluid and the linearized Bernoulli and kinematic boundary conditions at the surface, hence the equations governing ϕ_c and ζ_c are

$$\nabla^2 \phi_c = 0 \quad \text{for } z \leqslant 0, \tag{17}$$

$$\left(\frac{\partial}{\partial t} - \boldsymbol{V} \cdot \nabla_h\right) \phi_c + g\zeta_c = 0 \quad \text{on } z = 0, \tag{18}$$

and

$$\phi_{cz} - \left(\frac{\partial}{\partial t} - \boldsymbol{V} \cdot \nabla_h\right) \zeta_c = 0 \quad \text{on } z = 0. \tag{19}$$

Also, it is useful to note from (18) and (19) that $\phi_{cz} = O(\epsilon \phi_{cx}) = O(\epsilon^3)$.

Details of the analysis following Dysthe (1979) and Brinch-Nielsen (1985) are given in the Appendix. The analysis results in a dimensional equation valid to $O(\epsilon^4)$ in the form

$$\begin{aligned} \mathrm{i}\left[\frac{\partial}{\partial t} + c_{g0}\frac{\partial}{\partial x} - \boldsymbol{V} \cdot \nabla_h\right] B - \frac{(gk_0)^{1/2}}{8k_0^2}(B_{xx} - 2B_{yy}) - \frac{k_0^4}{2(gk_0)^{1/2}} B|B|^2 - k_0 \phi_{cx} B \\ = \frac{\mathrm{i}k_0^3}{4(gk_0)^{1/2}} B\left(BB_x^* - 6B_x B^*\right) + \frac{\mathrm{i}(gk_0)^{1/2}}{16k_0^3}(B_{xxx} - 6B_{yyx}) + k_0 \bar{\phi}_x B + P_1, \end{aligned} \tag{20}$$

where the $O(\epsilon^4)$ terms involving the current are

$$P_1 = \mathrm{i}k_0 \left(\frac{1}{2(gk_0)^{1/2}}\left[\frac{\partial}{\partial t} + c_{g0}\frac{\partial}{\partial x} - \boldsymbol{V} \cdot \nabla_h\right] \phi_{cx} - \phi_{cz}\right) B - \mathrm{i}\nabla_h \phi_c \cdot \nabla_h B,$$

and the wave-induced flow is described by equations (A 5), (A 17) and (A 18):

$$\left.\begin{aligned} &z < 0, \quad \nabla^2 \bar{\phi} = 0, \\ &z = 0, \quad \left(\frac{\partial}{\partial t} - (\boldsymbol{V} \cdot \nabla_h)\right) \bar{\phi} + g\bar{\zeta} = O(\epsilon^4), \\ &z = 0, \quad \frac{\partial \bar{\phi}}{\partial z} - \frac{k_0}{2}\left(\frac{k_0}{g}\right)^{1/2} \frac{\partial |B|^2}{\partial x} = O(\epsilon^4). \end{aligned}\right\} \tag{21}$$

In addition, the second-harmonic term is found to be

$$B_2 = \mathrm{i}\frac{k_0^6}{2(gk_0)^{3/2}} B^2|B|^2 + \frac{\mathrm{i}}{2(gk_0)^{1/2}}\left(BB_{yy} - B_y^2\right) \tag{22}$$

as in Brinch-Nielsen (1985), and the surface elevation terms are

$$\left.\begin{aligned} A &= \frac{\mathrm{i}k_0}{(gk_0)^{1/2}}\left[B - \frac{\mathrm{i}}{2k_0}B_x + \frac{1}{8k_0}^{2}(B_{xx} - 2B_{yy})\right] + \mathrm{i}\frac{k_0^5}{8(gk_0)^{3/2}}B|B|^2, \\ A_2 &= -\frac{k_0^2}{2g}\left[B^2 - \frac{2\mathrm{i}}{k_0}BB_x\right], \\ \text{and} \\ A_3 &= -\frac{3\mathrm{i}k_0^5}{8(gk_0)^{3/2}}B^3. \end{aligned}\right\} \tag{23}$$

The current does not enter into expressions (23) for the surface elevation directly at this order, since the first significant term for ζ would be of order $\nabla\phi\ (\nabla\cdot\boldsymbol{U}) \sim O(\epsilon^4)$ and for $\bar{\zeta}$ there is also an $O(\epsilon^4)\ \boldsymbol{U}^2$ term.

A dimensionless version of equation (20) valid to $O(\epsilon^4)$ (hereafter referred to as the CNLS^4 equation) is

$$\begin{aligned} &\mathrm{i}\overline{B}_T - \tfrac{1}{8}(\overline{B}_{\overline{X}\,\overline{X}} - 2\overline{B}_{\overline{Y}\,\overline{Y}}) - \tfrac{1}{2}\overline{B}|\overline{B}|^2 - \overline{B}\Phi_{c\overline{X}} \\ &\qquad = \frac{\mathrm{i}}{16}(\overline{B}_{\overline{X}\,\overline{X}\,\overline{X}} - 6\overline{B}_{\overline{Y}\,\overline{Y}\,\overline{X}}) + \overline{\Phi}_{\overline{X}}\overline{B} + \frac{\mathrm{i}}{4}\overline{B}(\overline{B}\,\overline{B}^*_{\overline{X}} - 6\overline{B}^*\overline{B}_{\overline{X}}) \\ &\qquad\qquad + \mathrm{i}\left(\tfrac{1}{2}\Phi_{c\overline{X}T} - \Phi_{cZ}\right)\overline{B} - \mathrm{i}\overline{\nabla}_h\Phi_c\cdot\overline{\nabla}_h\overline{B}, \end{aligned} \tag{24}$$

where $\overline{B} = k_0^2 B/(gk_0)^{1/2}$, $\Phi_c = k_0^2\phi_c/(gk_0)^{1/2}$, $\overline{\Phi} = k_0^2\bar{\phi}/(gk_0)^{1/2}$, $\overline{X} = k_0(x - \{c_{g0} - V_1\}t)$, $\overline{Y} = k_0(y + V_2 t)$, $Z = k_0 z$ and $T = (gk_0)^{1/2}t$. Dimensionless equations corresponding to (21), (22) and (23) are readily derived. Equation (24) agrees with that in Dysthe (1979) for $\phi_c \equiv 0$, except for certain factors of two arising from the present definition of B and $\bar{\phi}$, and for a slight error which has been noted in previous works. Comparing this equation to the $O(\epsilon^3)$ equation derived in the previous section we note that the non-dimensional current term $f(\overline{X}, \overline{Y}, T)$ there is equal to $\Phi_{c\overline{X}}$ and that all terms on the right-hand side of equation (24) are of $O(\epsilon^4)$. Equating the left-hand side of equation (24) to zero gives the $O(\epsilon^3)$ current-modified version of the cubic NLS equation; we will hereafter refer to this as the CNLS^3 equation.

4. A specific current: the surface current due to an internal wave

We choose to investigate the range of validity of the CNLS^3 and CNLS^4 equations in one horizontal dimension by using the surface current generated by an underlying internal wave, as discussed in detail in DPS. A simple model is used: the two-layer model for a stratified ocean. The frequency, wavelength and wavenumber of the internal wave are taken to be Ω, Λ and K respectively where $K = 2\pi/\Lambda$, $\Omega = O(\epsilon\omega_0)$ and $K = O(\epsilon k_0)$. Also, the phase speed of the internal wave $V_1 = \Omega/K$ is normally very much less than that of surface waves of the same wavenumber. The interface between the two fluids is perturbed slightly so that the problem may be linearized and a normal mode representation is taken for the velocity potentials in the upper and lower layers (depths h_1 and h_2 respectively), and the elevation ζ_c of the interface. Application of Laplace's equation, the linearized Bernoulli and kinematic boundary conditions (17)–(19), gives the dispersion relation which can be solved in the limit

$h_2 \to -\infty$ to obtain Ω^2:

$$\Omega^2 = \frac{gK(\rho_2 - \rho_1)}{\rho_1 - \rho_2 \coth K h_1}, \tag{25}$$

where ρ_1 and ρ_2 are the densities in the upper and lower layers respectively. Analytic forms for the surface elevation ζ_c and the velocity potential ϕ_c in the upper layer can be found which lead to a surface current of the form

$$\left.\frac{\partial \phi_c}{\partial \hat{x}}\right|_{z=0} = U_c \cos(K\hat{x} - \Omega t). \tag{26}$$

Here $\hat{x}$ is the coordinate parallel to x in the frame of reference where the water is stationary at depth. If we move into a frame of reference moving with the phase speed V_1 of the internal wave, the resulting current is appropriate for the current-modified NLS equations, i.e. let $x = \hat{x} - V_1 t$, so

$$\left.\frac{\partial \phi_c}{\partial x}\right|_{z=0} = U_c \cos(Kx) - V_1, \tag{27}$$

which is a slowly varying (if $K = O(\epsilon k_0)$), periodic, spatial current independent of time. We have $U_0 = -V_1$, a constant, and we consider currents where $U(x) - U_0 = U_c \cos(Kx)$ is relatively small. For presentation purposes, the space coordinate is given in units of $1/K$, whereas the time coordinate is non-dimensionalized with $(gK)^{1/2}$. Note that this non-dimensionalization for length based on the wavenumber, K, of the surface current is in contrast to that based on the wavenumber, k_0, of the carrier wave which leads to equations (8) and (24).

We consider initial conditions of a wavetrain of constant amplitude, with wavenumber k_0. This corresponds to surface waves generated by a passing gust of wind, where the waves that are generated are more or less uniform since they are all forced by the same wind for a similar duration. As shown by DPS, this initial condition has none of the special features of waves with constant absolute angular frequency, which have often been studied because of their analytical convenience (see, for example, Gargett & Hughes 1972). The plane-wave initial condition is more general, and with variations in the initial steepness, strength of current and initial wavenumber, provides a good test for the CNLS^3 and CNLS^4 equations. If we define $\delta = U_c/(g/k_0)^{1/2}$ and $\hat{V}_1 = V_1/(g/k_0)^{1/2}$ to be velocity ratio parameters relating basic velocity components of the surface current to the phase speed of the carrier wave in the absence of a current, we find that the non-dimensional current term $f(\overline{X}, \overline{Y}, T)$ in equation (8) takes the form

$$\delta \cos(Kx) = \delta \cos\left[\frac{K}{k_0}(\overline{X} + (\tfrac{1}{2} - \hat{V}_1)T)\right]. \tag{28}$$

This form for the current demonstrates the important parameters in the leading-order CNLS^3 equation. First, and probably most importantly, for our theory to be valid we require $\delta = O(\epsilon^2)$. Secondly, for the current to remain slowly varying, $K = O(\epsilon k_0)$. Thirdly, we note the presence of the $(\frac{1}{2} - \hat{V}_1)$ term in the phase of the current. The value $\hat{V}_1 = \frac{1}{2}$ corresponds to the mean value of the current being exactly equal and opposed to the group velocity of the carrier wave in the absence of a current. We expect a strong interaction between the current and the surface waves at this value of $\hat{V}_1$.

It is physically relevant to consider up to several hundred wavelengths of the short waves on one wavelength of an internal wave. For example, in an estuarine channel, experimental data are available for which $\lambda = 0.4\,\mathrm{m}$ and $\Lambda = 120\,\mathrm{m}$ giving $\Lambda/\lambda = 300$.

Here we could have a pycnocline with $h_1 = 6.0\,\mathrm{m}$ with density difference 2.5 parts per thousand say, and the surface current may have a maximum value of $0.04\,\mathrm{m\,s^{-1}}$. These physical values give $(\delta, \hat{V}_1) = (0.051, 0.414)$ and we hereafter refer to this as the 'standard case'. We also use for comparison an example of a stronger current with a maximum value of $0.08\,\mathrm{m\,s^{-1}}$, corresponding to $(\delta, \hat{V}_1) = (0.101, 0.414)$, and a 'longer' short-wave initial condition (that is, decreasing k_0) which gives $(\delta, \hat{V}_1) = (0.051, 0.262)$. Note that in figures 1 to 3 we have only taken $k_0/K = 20$ because, in order to obtain accurate solutions from the fully nonlinear potential solver that we use for comparison purposes, it is computationally impractical to consider many hundreds of wavelengths of short waves. However, this too is a physically relevant situation – for example, consider a greater density difference at a shallower pycnocline such as the freshwater having low salinity of 10 parts per thousand overlying sea water with salinity content of 35 parts per thousand with pycnocline depth of 0.77 m. Thus, our computations directly model the physical situation in which twenty wavelengths of a short wave arise on an 8 m internal wave with a maximum current of $0.047\,\mathrm{m\,s^{-1}}$. We expect that this still shows the generic features of solutions where $K = O(\epsilon k_0)$. These values of δ are $O(\epsilon^2)$ for values of ak of 0.2 to 0.3, which seem to be sensible values for this higher-order theory.

5. Results

5.1. *Numerical solution*

In order to solve the CNLS^3 equation, the split-step method used by Weidman & Herbst (1986) was used. The Fourier method they discussed was employed as we are concerned with a periodic surface current. The method was extended following Lo & Mei (1985) to solve the CNLS^4 equation. It was not difficult to extend these numerical methods to include the new current terms. There were two slight differences between the method employed here and that used by Lo & Mei (1985). First, Lo & Mei solved the equations in a transformed coordinate system owing to the generation of numerical noise in the original one; we did not find it necessary to do this as there was no significant numerical noise in our calculations. Secondly, Lo & Mei (1985) use a space derivative of $\bar{\phi}$ in their form for ζ given by their equation (2.12); we use the time derivative (given in this paper by rearrangement of equation (A 17) in the Appendix) and use a small time step in the numerical routine.

Results are presented as $K\zeta$ against $K\hat{x}$ at successive non-dimensional times $(gK)^{1/2}t$, increasing up the ordinate axis. The maximum and minimum values of the surface current are indicated by lines (– – ––) and (– · – · –) respectively. The full lines show surface profiles generated by the fully nonlinear code, and the dotted lines are results from the equation derived. Surface profiles for comparison are generated by finding ζ given by (16). Although the dependent computational variables are simply the modulation amplitude, B, of the short-wave velocity potential and the velocity potential of the induced current, the full detail of the free-surface shape and velocity field can be constructed to the same order of approximation using the relations (23). For the solution of the $O(\epsilon^3)$ CNLS^3 equation shown in figure 1, the profiles are given accurate to $O(\epsilon^2)$. In the remaining results which show solutions of the $O(\epsilon^4)$ CNLS^4 equation, profiles are given accurate to $O(\epsilon^3)$ (which includes the term $\bar{\zeta}$, surface elevation due to the mean flow current). In addition, fourth- and fifth-order Stokes wave terms are added. Although this is not entirely consistent, we expect these extra terms to show a better profile for the waves. The corresponding higher-order terms in the wave modulation that we are ignoring should be insignifi-

cant until close to the point of 'breaking'. Details for the construction of these terms can be found in Schwartz (1973). The elevation scale for figures 1 to 4 is given in the captions below the figures.

Relative computation times are of interest. As expected, the CNLS^3 equation is solved faster than the CNLS^4 equation-the latter taking about 2 minutes to run up to $(gK)^{1/2}t = 58$, with time step of 0.01 and 100 spatial Fourier modes. The fully nonlinear code, however, takes about 12 hours to run the same calculation to breaking at $(gK)^{1/2}t = 56$. The computations were done on a Sun Ultra 2/200.

5.2. *Discussion*

In order to see how well the CNLS^3 and CNLS^4 equations model the effect of the interaction between the surface current and the initially sinusoidal short waves, we compare surface profiles for $t > 0$ with solutions from the fully nonlinear numerical solver. Results are presented for times large enough for either the full nonlinear code to predict 'breaking', i.e. there are regions of very high surface curvature where there are insufficient discretization points to give results within the accuracy required†, or else until the CNLS^3 and CNLS^4 solutions cease to be accurate for some reason, such as the waves no longer being part of a single wavetrain which is the case in the region between two caustics after a focus, where there are three overlapping wavetrains, or where there are abrupt changes in wave properties.

Since we have a high-order approximation, we are considering waves that are approaching breaking. The wave steepness parameter, ak, becomes hard to define from the wave profile due to the crest–trough asymmetry combined with the relatively rapid variation of both wave height, crest to trough or vice versa, and of wavelength however defined. The approximate equations can satisfactorily describe waves which vary significantly from crest to crest. This success can best be accounted for by noting that a good measure of the wave's length scale is $1/k$, and a wavelength, $2\pi/k$, is relatively long compared to $1/k$, i.e. $(2\pi)^{-1} = 0.159\ldots$ is sufficiently small. Hence we consider the maximum slope of the water surface. This equals ak for waves of low steepness, but is not accurate for nonlinear waves of $ak > 0.1$. For example, the difference between ak and maximum slope at $ak = 0.2$ is 2%, and at $ak = 0.43$ is 24%. These values have been found by solving the full nonlinear water wave equations to obtain accurate surface profiles for increasing values of ak, and measuring the maximum wave slope. They are for steady waves – for unsteady wave breaking, surface slopes pass 90°. For this reason, the condition for 'breaking' incorporated into the code which solves the CNLS^3 and CNLS^4 equations is to halt the calculations when the slope $\mathrm{d}\zeta/\mathrm{d}x$ exceeds a value at which the waves could be expected to evolve to breaking. We take this value to correspond to $ak = 0.40$ which gives a maximum slope $\mathrm{d}\zeta/\mathrm{d}x = 0.462$. We expect waves of maximum slopes above this value to become unstable due to Tanaka's (1983) instability, and then to break, since the instability is localized near the wave crest.

Figure 1 shows results from solving the CNLS^3 equation with conditions for the 'standard case' when the short waves initially have steepness $ak_0 = 0.10$. In this case, the fully nonlinear code predicts breaking at $(gK)^{1/2}t = 56$. One wavelength of the surface current is shown. For $(gK)^{1/2}t < 20$, comparison with the fully nonlinear results is good, but for later times the CNLS^3 equation does not accurately model the speed of the group of steepening waves. However, for all times, the less steep

† The numerical discretization can be enhanced to enable wave overturning to be described, but such extra precision is not warranted in this case.

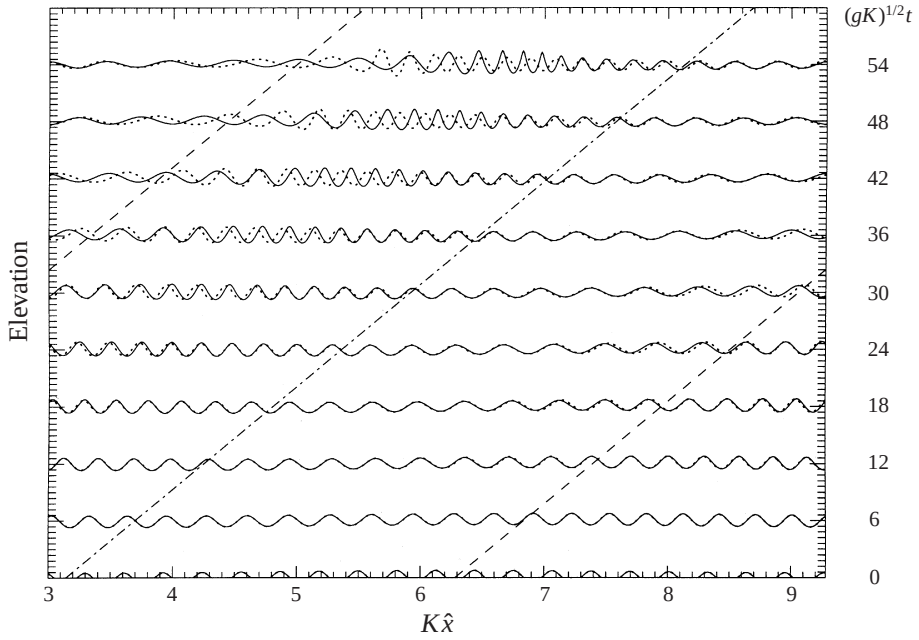

FIGURE 1. Surface profiles comparing the $O(\epsilon^3)$ CNLS^3 solutions (dotted line) with results from the fully nonlinear potential solver (full line), for the 'standard case': each small interval on the vertical axis represents an elevation $K\zeta = 0.005$ which is equivalent to a vertical exaggeration of approximately 10 : 1, time, t, is non-dimensionalized with $(gK)^{1/2}$, $(\delta, \gamma) = (0.051, 2.416)$ and initial steepness $ak_0 = 0.10$. Breaking occurred for the fully nonlinear calculations at $(gK)^{1/2}t = 56$.

waves are modelled moderately well. We would not expect the CNLS^3 equation to model the speed of the steep group of waves as it does not include terms which increase group velocity as the steepness of the waves increases, i.e. the B^2B_x term in the CNLS^4 equation. In this case the CNLS^3 solution reached $ak = 0.40$ just after $(gK)^{1/2}t = 58$.

Figure 2 compares the same results from the fully nonlinear solver to results from the CNLS^4 equation. Results are now very encouraging. Away from the steep group of waves, the CNLS^4 equation models the waves very accurately for all times. The region of steep waves is modelled to graphical accuracy up to $(gK)^{1/2}t \sim 35$. For later times, the steep waves predicted by the CNLS^4 are slower than those from the fully nonlinear potential solver. One reason for the breakdown of the solution is that the derivation of the CNLS^4 equation is based on the assumption that the waves are all part of a slowly varying wavetrain; however, at $K\hat{x} \sim 2\pi$, $(gK)^{1/2}t = 54$ we see that wavenumber changes are rapid, thus causing the solutions from the CNLS^4 equation to deteriorate. 'Breaking' is predicted by the CNLS^4 equation just after $(gK)^{1/2}t = 58$.

Figure 3 shows results from the 'standard case' when the short waves have initial steepness $ak_0 = 0.01$. Here, the fully nonlinear code does not predict breaking within the time considered. As is discussed in DPS, in this case the interaction of the current with the short surface waves is well predicted by linear ray theory. The waves are focused at $(gK)^{1/2}t \sim 60$ and at later times there is a region of three overlapping wavetrains between two caustics. The caustic positions predicted by linear ray theory are shown by the long dashes (— — —) on figure 3. Between the caustics, the waves have become more irregular. As the derivation of the nonlinear Schrödinger equation

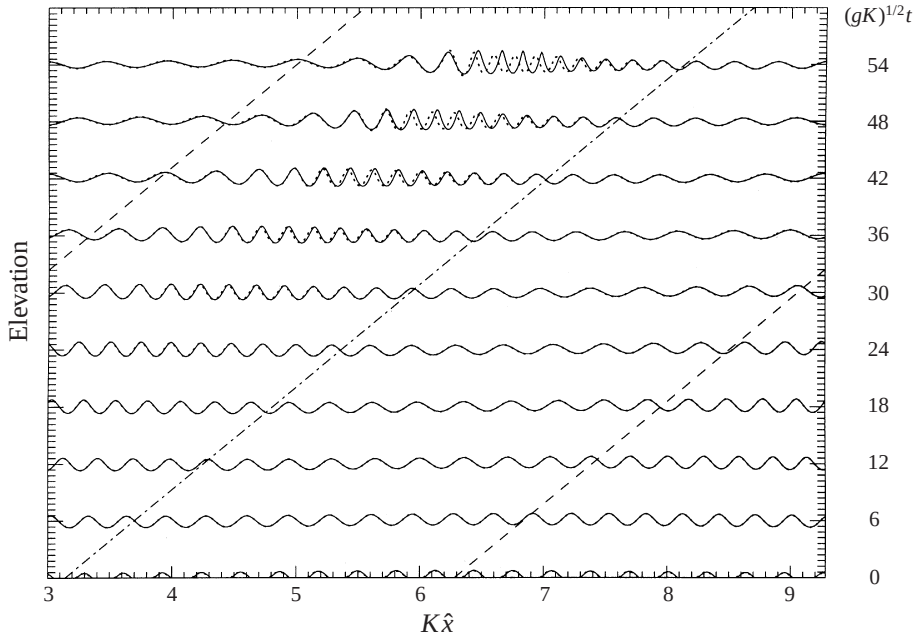

FIGURE 2. Surface profiles comparing the $O(\epsilon^4)$ CNLS^4 solutions (dotted line) with results from the fully nonlinear potential solver (full line), for the 'standard case': each small interval on the vertical axis represents an elevation $K\zeta = 0.005$ which is equivalent to a vertical exaggeration of approximately 10 : 1, time, t, is non-dimensionalized with $(gK)^{1/2}$, $(\delta, \gamma) = (0.051, 2.416)$ and initial steepness $ak_0 = 0.10$. Breaking occurred for the fully nonlinear calculations at $(gK)^{1/2}t = 56$.

is based on the assumption that the waves form part of a single, slowly varying wavetrain, we would not expect any prediction by the CNLS^4 equation in this region of overlapping wavetrains to be accurate, and this is indeed the case. Away from this region, where the waves are a single wavetrain, the results compare relatively well. However, the fully nonlinear results show a short, steep group of waves generated at the focus ($(gK)^{1/2}t \sim 60$), which propagates up the left-hand caustic. This group is not modelled accurately by the CNLS^4 equation once the focal region is passed owing to the fast variation of wave properties corresponding to three superposed wavetrains; however, the group's creation in the focal region is well described by the CNLS^4 equation.

An additional assumption made in the analysis leading to the CNLS^3 and CNLS^4 equations is that the current variation must be small. In non-dimensional terms, for the sinusoidal current, this means that $\delta = O(\epsilon^2)$. Figure 4 shows the final stages before wave breaking for a current twice as strong as that considered previously, and with an initial condition as considered in figure 1, i.e. $ak_0 = 0.10$ (thus doubling δ). The fully nonlinear code predicts breaking at $(gK)^{1/2}t = 33$, a time considerably earlier than with a weaker current – an observation which can be explained in terms of the time to focus predicted by the linear ray theory (see DPS for further discussion). The modelling by the CNLS^4 equation is still good for this stronger current, with the longer less steep waves being very well represented, although, as before, the steeper, short waves are predicted by the CNLS^4 equation to travel slower. Note that this figure shows only half a wavelength of the surface current. The fully nonlinear results show that the wave which 'breaks' is at the start of the group of steep waves. The CNLS^4

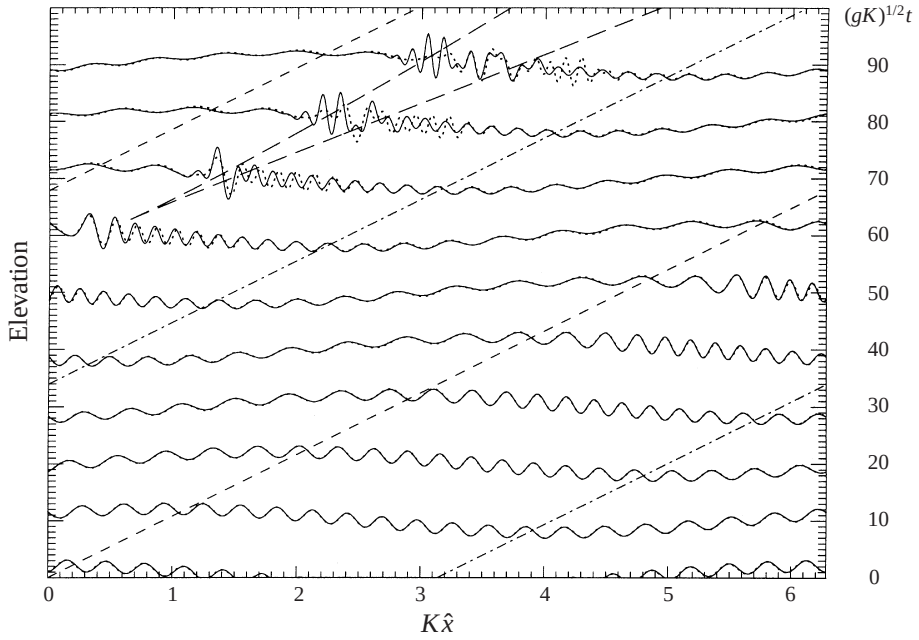

FIGURE 3. Surface profiles comparing the $O(\epsilon^4)$ CNLS^4 solutions (dotted line) with results from the fully nonlinear potential solver (full line), for the 'standard case', the position of the caustics predicted by linear ray theory being indicated by long dashes: each small interval on the vertical axis represents an elevation $K\zeta = 0.0005$ which is equivalent to a vertical exaggeration of approximately 100 : 1, time, t, is non-dimensionalized with $(gK)^{1/2}$, $(\delta, \gamma) = (0.051, 2.416)$ and initial steepness $ak_0 = 0.01$. No breaking occurred.

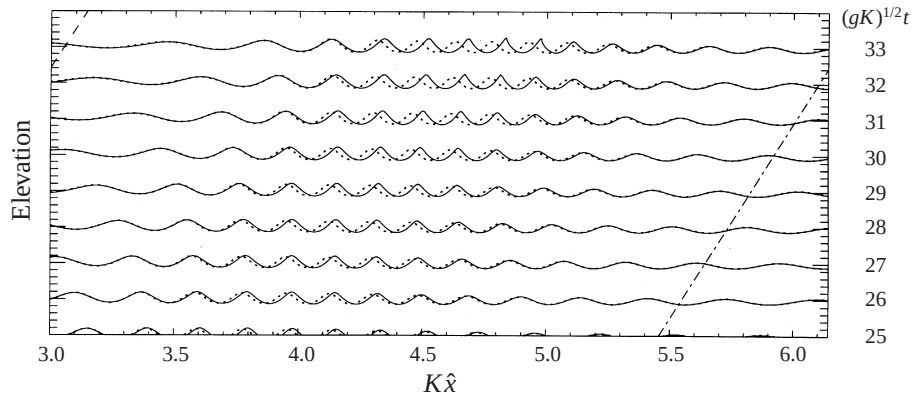

FIGURE 4. Final stages before wave breaking comparing the $O(\epsilon^4)$ CNLS^4 solutions (dotted line) with results from the fully nonlinear potential solver (full line), for a stronger current: each small interval on the vertical axis represents an elevation $K\zeta = 0.01$ which is equivalent to a vertical exaggeration of approximately 3 : 1, time, t, is non-dimensionalized with $(gK)^{1/2}$, $(\delta, \gamma) = (0.101, 2.416)$ and initial steepness $ak_0 = 0.10$. Breaking occurred for the fully nonlinear calculations at $(gK)^{1/2}t = 33$.

equation cannot be expected to model the final evolution before breaking, just as the small-amplitude perturbation for Stokes waves fails to describe the steepest waves.

In DPS, figure 13 shows the time of breaking against initial steepness for the standard case, a stronger current and when initially 'longer' short waves are taken.

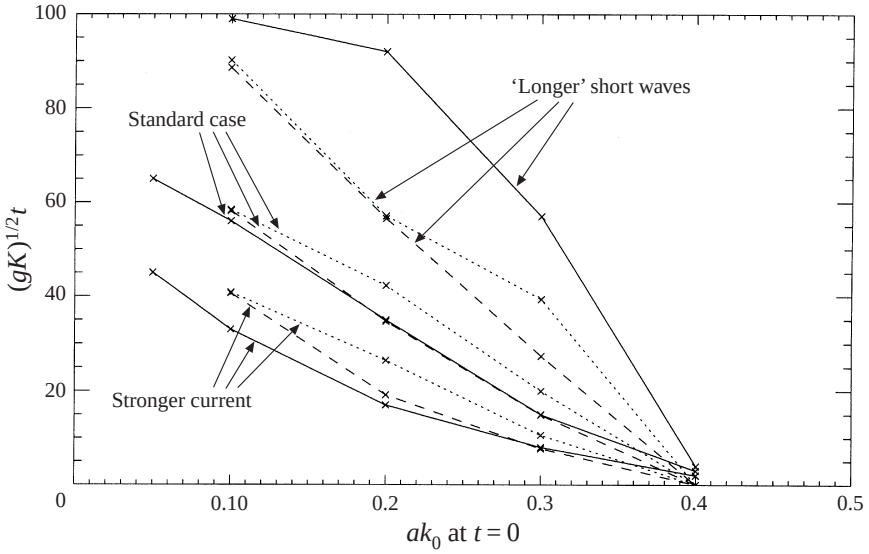

FIGURE 5. Time of breaking against initial steepness of the short waves: the solid line shows fully nonlinear results, the dotted line shows the CNLS^3 results, and the dashed line shows the CNLS^4 results. The crosses indicate where the waves have reached 'breaking' – corresponding to regions of high curvature in the case of the fully nonlinear calculations, and a maximum wave slope of 0.462 in the weakly nonlinear calculations.

Time $(gK)^{1/2}t$	Fully nonlinear	CNLS^4
0	0.10	0.10
10	0.12	0.12
20	0.15	0.15
30	0.19	0.18
40	0.24	0.23
50	0.34	0.31
52	0.39	0.36
54	0.45	0.43
'breaking'	$(gK)^{1/2}t = 56$	$(gK)^{1/2}t = 58$

TABLE 1. Maximum slope (to 2 decimal places) for the 'standard case' from the fully nonlinear numerical solver and the CNLS^4 equation with $ak_0 = 0.10$ initially, $(\delta, \gamma) = (0.051, 2.416)$.

Here figure 5 shows the same results along with the CNLS^3 equation (dotted line) and CNLS^4 equation (dashed line) predictions for breaking – that is when $ak = 0.40$. We see that the prediction for the time of breaking for the CNLS^4 equation for the standard case is very accurate. For a stronger current, predicted times for breaking are less accurate, as expected. Also for 'longer' short waves, the CNLS^4 equation predicts breaking to occur much earlier than is predicted by the fully nonlinear code. This is because K/k_0 has increased, thus making the surface current relatively less slowly varying – see the non-dimensional form for the current given by (28) for verification of this. For almost all cases, the CNLS^3 equation predicts breaking later than the CNLS^4 equation.

Table 1 compares values of maximum slope of the waves with time for the fully nonlinear solver to that predicted by the CNLS^4 equation, for the 'standard case'

with an initial condition $ak_0 = 0.10$ as shown in figure 2. This demonstrates that the weakly nonlinear theory leading to the CNLS[4] equation does not predict quite as large steepnesses as that predicted by the fully nonlinear code, as we could expect from a theory that neglects fully nonlinear terms which are important in regions where waves are both steepening and close to breaking.

6. Conclusion

In this paper we have derived a current-modified nonlinear Schrödinger equation. Two forms of the equation have been discussed: one valid to $O(\epsilon^3)$, and one to $O(\epsilon^4)$, where $\epsilon = ak$ is a measure of the steepness. As with the standard nonlinear Schrödinger equation, solutions are valid when waves form part of a slowly varying wavetrain, and solutions break down when the variation of wave properties is too fast. In addition, the current-modified nonlinear Schrödinger equation is valid for currents that are large scale relative to the short surface waves and have a small, slow variation from a mean value.

In order to check the validity of the equation numerically in one horizontal dimension, we compare surface profiles with those obtained from a fully nonlinear potential solver. We have chosen for comparison purposes to study the evolution of waves on a large-scale current (such as may be due to an underlying internal wave) from an initial constant-wavenumber wavetrain. We find that the $O(\epsilon^3)$ equation compares moderately well, and the $O(\epsilon^4)$ equation compares very well, up to the point where weakly nonlinear theory is no longer valid, i.e. when the wave becomes almost steep enough to break.

For the particular example of a surface current chosen, we have identified situations in which solutions to the new equation compare well, and others in which they become less accurate. In addition, we have made an investigation into the 'time of breaking'. For solutions of the current-modified nonlinear Schrödinger equation, we have specified a critical slope criterion for 'breaking', which we have taken to be $ak = 0.40$, $\mathrm{d}\zeta/\mathrm{d}x = 0.462$, whereas the fully nonlinear code predicts 'breaking' when there are insufficient discretization points in regions of high curvature (such as at a sharp or overturning crest) to give results within the accuracy required.

Further studies could follow the work of Trulsen & Dysthe (1996, 1997) to include the extra terms to make the equation valid for a broader bandwidth, and observe the nature of the frequency downshift in the presence of a current. Also valuable would be a comparison of the results from our numerical calculations with those from experiments, as in Lo & Mei (1985) and Trulsen, Stansberg & Velarde (1999) for the case when no current is present, and as Bakhanov *et al.* (1997) have done for the CNLS[3] equation. Another form of current that is of interest has shear in the vertical. That type of current has been discussed by Pullin & Grimshaw (1986) and, for the particular case of Dysthe's (1979) MNLS equation, by Dhar & Das (1994).

We would like to acknowledge the financial support of the DERA; and both Alice Donato and Mark Jervis for their work on the fully nonlinear code.

Appendix

The analysis involves the substitution of the expansions (15) and (16) for ϕ and ζ in equations (13) and (14). Fourier coefficients are equated. Any remaining 'slow variation' terms are real and only required to $O(\epsilon^3)$; these govern the modulation of the potential $\bar{\phi}$ due to waves.

In two dimensions, Laplace's equation leads to a useful result which is used throughout the analysis:

$$B_z = -\mathrm{i}B_x - \frac{1}{2k_0}B_{yy} - \frac{\mathrm{i}}{2k_0^2}B_{xyy} + O(\epsilon^5). \tag{A 1}$$

This is can proved by using an iterative procedure. First, directly from Laplace's equation and the $\mathrm{e}^{\mathrm{i}\theta}$ term in (15)

$$B_z + \mathrm{i}B_x = -\frac{1}{2k_0}\nabla^2 B = O(\epsilon^3). \tag{A 2}$$

Differentiation with respect to x and z, and a little manipulation gives

$$B_{zz} + B_{xx} = \frac{\mathrm{i}}{k_0}\frac{\partial}{\partial x}\nabla^2 B + O(\epsilon^5), \tag{A 3}$$

so

$$\nabla^2 B = B_{yy} + \frac{\mathrm{i}}{k_0}B_{xyy} + O(\epsilon^5), \tag{A 4}$$

where the suffix notation for derivatives is being used. Consideration of both equations (A 2) and (A 4) leads to equation (A 1). This relation also holds for B_2. Evaluating the slow modulation terms gives

$$\nabla^2\bar{\phi} = 0 \quad \text{for } z < 0. \tag{A 5}$$

We now go through the terms in equation (13) one by one, and evaluate their contribution at $z = 0$. This generates a nonlinear, current-modified Schrödinger equation, accurate to $O(\epsilon^4)$. Equation (14) is used to evaluate the surface elevation ζ.

The $\mathrm{L}\phi$ term gives a contribution

$$\mathrm{L}\phi = \mathrm{L}\bar{\phi} + \left[\left\{\tfrac{1}{2}(B_{tt} - 2(\boldsymbol{V}\cdot\nabla_h)B_x + (\boldsymbol{V}\cdot\nabla_h)^2 B) - \frac{g}{4k_0}\left(B_{yy} - \frac{\mathrm{i}}{k_0}B_{xyy}\right)\right.\right.$$
$$\left.\left. -\mathrm{i}(gk_0)^{1/2}(B_t + c_{g0}B_x - (\boldsymbol{V}\cdot\nabla_h)B)\right\}\mathrm{e}^{\mathrm{i}\theta} + \mathrm{c.c.}\right] - \left[gk_0 B_2 \mathrm{e}^{2\mathrm{i}\theta} + \mathrm{c.c.}\right]. \tag{A 6}$$

Dysthe (1979) finds no contribution from the second term in equation (13). However, Brinch-Nielsen finds a second-harmonic $O(\epsilon^4)$ term here; we agree, and in addition, a current term is present. We find

$$\zeta\mathrm{L}\frac{\partial\phi}{\partial z} = \left[-Ak_0^2\left(\frac{(gk_0)^{1/2}}{2}\phi_{cx}B + \frac{k_0^3}{4}B|B|^2\right)\mathrm{e}^{2\mathrm{i}\theta} + \mathrm{c.c.}\right]$$
$$+ \text{ slow variation terms of } O(\epsilon^4). \tag{A 7}$$

It is next useful to find a form for $(\nabla\phi)^2$ in order to evaluate many of the remaining terms:

$$(\nabla\phi)^2 = \mathrm{e}^{2k_0 z}\left(k_0^2|B|^2 + \mathrm{i}k_0(BB_x^* - B^*B_x) + B_xB_x^*\right) + \tfrac{1}{2}B_yB_y^* - \tfrac{1}{2}(BB_{yy}^* + B^*B_{yy})$$
$$+(\nabla_h\phi_c)^2 + \left[(\mathrm{i}k_0 B(\mathrm{M}\bar{\phi} + \mathrm{M}\phi_c) + \nabla_h B\cdot\nabla_h\phi_c)\mathrm{e}^{k_0 z}\mathrm{e}^{\mathrm{i}\theta} + \mathrm{c.c.}\right]$$
$$+\left[\tfrac{1}{4}(B_y^2 - BB_{yy})\mathrm{e}^{2k_0 z}\mathrm{e}^{2\mathrm{i}\theta} + \mathrm{c.c.}\right] \tag{A 8}$$

where

$$\mathrm{M} = \frac{\partial}{\partial x} - \mathrm{i}\frac{\partial}{\partial z}.$$

This allows us to evaluate the third term in equation (13):

$$\left(\frac{\partial}{\partial t} - \boldsymbol{V}\cdot\nabla_h\right)(\nabla\phi)^2 = \left[\left\{k_0(gk_0)^{1/2}B(\mathrm{M}\phi_c + \mathrm{M}\bar{\phi}) + \mathrm{N}(\phi_c, B)\right\}\mathrm{e}^{\mathrm{i}\theta} + \mathrm{c.c.}\right]$$
$$+ \left[\left\{-\mathrm{i}\frac{(gk_0)^{1/2}}{2}(B_y^2 - BB_{yy})\right\}\mathrm{e}^{2\mathrm{i}\theta} + \mathrm{c.c.}\right]$$
$$-\frac{(gk_0)^{1/2}k_0}{2}\frac{\partial|B|^2}{\partial x} + \text{slow variation terms of } O(\epsilon^4) \quad \text{(A 9)}$$

where

$$\mathrm{N}(\phi_c, B) = \mathrm{i}k_0 B\left(\frac{\partial}{\partial t} - (\boldsymbol{V}\cdot\nabla_h)\right)\phi_{cx} - \mathrm{i}(gk_0)^{1/2}\left(\tfrac{3}{2}\phi_{cx}B_x + \phi_{cy}B_y\right).$$

We now move on to evaluate the terms of Q_3. The first term has no contribution to the relevant order. The second term generates an $O(\epsilon^4)$ term:

$$\tfrac{1}{2}\nabla\phi\cdot\nabla(\nabla\phi)^2 = \left[\frac{k_0^3}{2}B\left(k_0|B|^2 + 2\mathrm{i}(BB_x^* - B^*B_x)\right)\mathrm{e}^{\mathrm{i}\theta} + \mathrm{c.c.}\right], \quad \text{(A 10)}$$

and the third term contributes

$$\zeta\left(\frac{\partial}{\partial t} - \boldsymbol{V}\cdot\nabla_h\right)\frac{\partial}{\partial z}((\nabla\phi)^2) = \left[-\mathrm{i}\frac{k_0^3}{2}B\frac{\partial|B|^2}{\partial x}\mathrm{e}^{\mathrm{i}\theta} + \mathrm{c.c.}\right] + \left[\mathrm{i}\frac{k_0^3}{2}\phi_{cx}B^2\mathrm{e}^{2\mathrm{i}\theta} + \mathrm{c.c.}\right]$$
$$+ \text{slow variation terms of } O(\epsilon^4). \quad \text{(A 11)}$$

Dysthe (1979) neglects all terms of Q_4. There is an $O(\epsilon^4)$ term present, but it is a second harmonic and therefore does not alter Dysthe's analysis. For completeness, we state

$$Q_4 = \tfrac{1}{6}\zeta^3\frac{\partial^3}{\partial z^3}(\mathrm{L}\phi) + \tfrac{1}{2}\zeta^2\frac{\partial}{\partial z}\left(\frac{\partial}{\partial t} - \boldsymbol{V}\cdot\nabla_h\frac{\partial}{\partial x}\right)((\nabla\phi)^2) + \tfrac{1}{2}\zeta\frac{\partial}{\partial z}\left(\nabla\phi\cdot\nabla(\nabla\phi)^2\right). \quad \text{(A 12)}$$

Only the third term gives any contribution to the relevant order:

$$\tfrac{1}{2}\zeta\frac{\partial}{\partial z}\left(\nabla\phi\cdot\nabla(\nabla\phi)^2\right) = \left[\mathrm{i}\frac{3k_0^6}{4(gk_0)^{1/2}}B^2|B|^2\mathrm{e}^{2\mathrm{i}\theta} + \mathrm{c.c.}\right]$$
$$+ \text{slow variation terms of } O(\epsilon^4). \quad \text{(A 13)}$$

Substitution of equations (A 6)–(A 13) in equation (13) and equating the $O(\mathrm{e}^{\mathrm{i}\theta})$ coefficients leads to an equation for the complex potential B, valid up to $O(\epsilon^4)$:

$$\mathrm{i}(gk_0)^{1/2}(B_t + c_{g0}B_x - (\boldsymbol{V}\cdot\nabla_h)B)$$
$$-\tfrac{1}{2}(B_{tt} - 2(\boldsymbol{V}\cdot\nabla_h)B_t + (\boldsymbol{V}\cdot\nabla_h)^2B) + \frac{g}{4k_0}B_{yy} - k_0(gk_0)^{1/2}\phi_{cx}B - \frac{k_0^4}{2}B|B|^2$$
$$= -\mathrm{i}k_0(gk_0)^{1/2}\phi_{cz}B - \frac{\mathrm{i}g}{4k_0^2}B_{xyy} + \mathrm{i}k_0^3B(BB_x^* - B^*B_x)$$
$$+ k_0(gk_0)^{1/2}\mathrm{M}\bar{\phi}B + \mathrm{N}(\phi_c, B) - \mathrm{i}\frac{k_0^3}{2}B\frac{\partial|B|^2}{\partial x}. \quad \text{(A 14)}$$

Iterating this equation to remove the B_{tt} and B_{xt} terms leads to the $O(\epsilon^3)$ left-hand side of the equation

$$\mathrm{i}(gk_0)^{1/2}(B_t + c_{g0}B_x - (\boldsymbol{V}\cdot\nabla_h)B) - \frac{g}{8k_0}(B_{xx} - 2B_{yy}) - k_0(gk_0)^{1/2}B\phi_{cx} - \frac{k_0^4}{2}B|B|^2 \tag{A 15}$$

and the $O(\epsilon^4)$ right-hand side is

$$\frac{\mathrm{i}g}{16k_0^2}\left(B_{xxx} - 6B_{xyy}\right) + \mathrm{i}\frac{k_0^3}{4}B\left(BB_x^* - 6B^*B_x\right) + k_0(gk_0)^{1/2}B\bar{\phi}_x + (gk_0)^{1/2}$$
$$\times\left[\mathrm{i}k_0\left\{\frac{1}{2(gk_0)^{1/2}}\left(\frac{\partial}{\partial t} + c_{g0}\frac{\partial}{\partial x} - (\boldsymbol{V}\cdot\nabla_h)\right)\phi_{cx} - \phi_{cz}\right\} - \mathrm{i}\nabla_h\phi_c\cdot\nabla_h B\right]. \tag{A 16}$$

Simplification and non-dimensionalization, as in Dysthe (1979), leads to equation (24).

Equating coefficients of $O(\mathrm{e}^{2\mathrm{i}\theta})$ in (13) leads to a form for B_2 given by (22) and finally, evaluation of the slow modulation terms give boundary conditions for $\bar{\phi}$:

$$z = 0, \quad \left(\frac{\partial}{\partial t} - (\boldsymbol{V}\cdot\nabla_h)\right)\bar{\phi} + g\bar{\zeta} = O(\epsilon^4), \tag{A 17}$$

$$z = 0, \quad \frac{\partial\bar{\phi}}{\partial z} - \frac{k_0}{2}\left(\frac{k_0}{g}\right)^{1/2}\frac{\partial|B|^2}{\partial x} = O(\epsilon^4). \tag{A 18}$$

REFERENCES

Ablowitz, M. J. & Herbst, B. M. 1990 On the homoclinic structure and numerically induced chaos for the nonlinear Schrödinger equation. *SIAM J. Appl. Maths* **50**, 339–351.

Bakhanov, V. V., Bogatyrev, S. D., Kazakov, V. I. *et al.* 1997 Laboratory investigations of nonlinear surface wave transformation in a field of two-dimensionally inhomogeneous currents. *Intl. Geoscience & Remote Sensing Sympos. Proc.* **I**, 350–352.

Bakhanov, V. V., Kemarskaya, O. N., Pozdnyakova, V. I. *et al.* 1996 Evolution of surface waves of finite amplitude in field of inhomogeneous current. *Intl. Geoscience & Remote Sensing Sympos. Proc.* **I**, 609–611.

Bretherton, F. P. & Garrett, C. J. R. 1968 Wavetrains in inhomogeneous moving media. *Proc. R. Soc. Lond.* A **302**, 529–554.

Brinch-Nielsen, U. 1985 Slowly modulated, weakly nonlinear gravity waves – fourth order evolution equations and stability analysis. MSc thesis, Tech. Univ. Denmark, pp. 99–109.

Davey, A. & Stewartson, K. 1974 On three-dimensional packets of surface waves. *Proc. R. Soc. Lond.* A **338**, 101–110.

Dhar, A. K. & Das, K. P. 1994 Stability analysis from fourth order evolution equation for small but finite amplitude interfacial waves in the presence of a basic current shear. *J. Austral. Math. Soc.* B **35**, 348–365.

Dold, J. W. 1992 An efficient surface-integral algorithm applied to unsteady gravity waves. *J. Comput. Phys.* **103**, 90–115.

Dold, J. W. & Peregrine, D. H. 1986 An efficient boundary-integral method for steep unsteady water waves. In *Numerical Methods for Fluid Dynamics II* (ed. K. W. Morton & M. J. Baines), pp. 671–679. Oxford University Press.

Donato, A. N., Peregrine, D. H. & Stocker, J. R. 1999 The focussing of surface waves by internal waves. *J. Fluid Mech.* **384**, 27–58 (referred to herein as DPS).

Dysthe, K. B. 1979 Note on the modification to the nonlinear Schrödinger equation for application to deep water waves. *Proc. R. Soc. Lond.* A **369**, 105–114.

GARGETT, A. E. & HUGHES, B. A. 1972 On the interaction of surface and internal waves. *J. Fluid Mech.* **52**, 179–191.

HASIMOTO, H. & ONO, H. 1972 Nonlinear modulation of gravity waves. *J. Phys. Soc. Japan.* **33**, 805–811.

JONSSON, J. J. 1990 Wave-current interactions. In *The Sea* (ed. B. le Mehaute & D. M. Haine), pp. 65–120. Wiley-Interscience.

LAMB, H. 1932 *Hydrodynamics*, 6th Edn, Chap. IX, pp. 417–420. Cambridge University Press.

LO, E. & MEI, C. C. 1985 Numerical study of water-wave modulation. *J. Fluid Mech.* **150**, 395–415.

LONGUET-HIGGINS, M. S. & STEWART, R. W. 1964 Radiation stress in water waves, a physical discussion with application. *Deep-Sea Res.* **11**, 529–562.

PEREGRINE, D. H. 1976 Interaction of water waves and currents. *Adv. Appl. Mech.* **16**, 9–117.

PULLIN, D. I. & GRIMSHAW, R. H. J. 1986 Stability of finite amplitude interfacial waves. Part 3. The effect of a basic current shear for one dimensional instabilities. *J. Fluid Mech.* **172**, 277–306.

SCHWARTZ, L. W. 1973 Computer extension and analytic continuation of Stokes expansion for gravity waves. *J. Fluid Mech.* **62**, 553–578.

TANAKA, M. 1983 The stability of steep gravity waves. *J. Phys. Soc. Japan* **52**, 3047–3055.

TRULSEN, K. & DYSTHE, K. B. 1996 A modified nonlinear Schrödinger equation for broader bandwidth gravity waves on deep water. *Wave Motion* **24**, 281–289.

TRULSEN, K. & DYSTHE, K. B. 1997 Frequency downshift in three-dimensional wave trains. *J. Fluid Mech.* **352**, 359–373.

TRULSEN, K., STANSBERG, C. T. & VELARDE, M. G. 1999 Laboratory evidence of three-dimensional frequency downshift of waves in a long tank. *Phys. Fluids* **11**, No.1.

WEIDMAN, J. A. C. & HERBST, B. M. 1986 Split-step methods for the solution of the nonlinear Schrödinger equation. *SIAM J. Numer. Anal.* **23**, 485–507.

WHITHAM, G. B. 1965 A general approach to linear and non-linear dispersive waves using a Lagrangian. *J. Fluid Mech.* **22**, 273–283.

WHITHAM, G. B. 1967 Non-linear dispersion of water waves. *J. Fluid Mech.* **27**, 399–412.

YUEN, H. C. & LAKE, B. M. 1982 Nonlinear dynamics of deep-water gravity waves. *Adv. Appl. Mech.* **22**, 67–229.

ZAKHAROV, V. E. 1968 Stability of periodic waves of finite amplitude on the surface of a deep water fluid. *J. Appl. Mech. Tech. Phys.* (*Engl. Transl.*) **2**, 190–194.